

## Stabilization, Selection, and Tracking of Unstable Patterns by Weak Spatial Perturbations

Peng-Ye Wang,<sup>1,2</sup> Ping Xie,<sup>1</sup> Jian-Hua Dai,<sup>1</sup> and Hong-Jun Zhang<sup>1,2</sup>

<sup>1</sup>Laboratory of Optical Physics, Institute of Physics & Center for Condensed Matter Physics,  
Chinese Academy of Sciences, P.O. Box 603, Beijing 100080, China

<sup>2</sup>CCAST (World Laboratory), P.O. Box 8730, Beijing 100080, China

(Received 22 May 1997; revised manuscript received 13 March 1998)

A spatial perturbation method for the stabilization of an unstable state of a pattern forming system is presented. The perturbation, as a weak driving signal, mimics the target pattern. Stabilization, selection, and tracking of unstable rolls, squares, hexagons, and honeycombs are demonstrated by numerical simulations through the example of an optical system. The application of an external spatial perturbation also results in critical slowing down and resonant phenomenon. [S0031-9007(98)06218-8]

PACS numbers: 47.54.+r, 05.45.+b, 42.65.Sf

Since the pioneering work of Ott, Grebogi, and Yorke (OGY) [1], considerable efforts have been made to suppress temporal disorder in chaotic regimes. In the past few years several methods have been proposed. The main technique (OGY method) is to stabilize one of the unstable periodic orbits embedded in the chaotic attractor based on the determination of the stable and unstable directions in the Poincaré section [1–5]. Another procedure is to introduce a self-controlling feedback [6,7]. The third important and effective method is to modulate a system parameter with a small periodic perturbation or to add a weak periodic forcing to the system [8–14]. The OGY method is rigorously proved to be valid for every system in general cases, while the self-controlling feedback method and the perturbation method are more suitable for experiments in practical systems, although the underlying dynamics is not so clear.

Early efforts toward control of spatiotemporal dynamics have been made by using the extension of the OGY algorithm [15,16]. Since then suppressions of spatiotemporal disorder in chaotic regimes have been investigated in different systems [17,18]. Recently, Lu *et al.* [19] extended the Pyragas method [6] to perform spatiotemporal control in an optical model which displays phenomena, such as pattern formation [20], common to many spatially extended systems. Stabilizing and manipulating unstable spatial states is closely related to the control of spatiotemporal instabilities. Most recently Martin *et al.* [21] developed a Fourier space technique to stabilize and track unstable patterns in a mean-field model for a two-level medium in an optical cavity. In this Letter, we present a nonfeedback technique which allows us to stabilize, select, and track such unstable spatial patterns. Our method is based on weak perturbations to the system in the spatial dimensions. The perturbation, as a weak spatial driving signal, mimics the target pattern, which is similar to the approaches in controlling temporal chaos by modulating a system parameter or adding a weak periodic forcing to the system [8–14]. It is important that our nonfeedback technique can be very easily realized in practical spatially

extended systems. For example, in an optical system both the amplitude and the phase of the field can be spatially perturbed with an absorptive or a dispersive optical mask. On the other hand, spatial perturbations widely and naturally exist in the dynamics of some growth, diffusion, and convection processes, such as pattern formation in epitaxial growth on surfaces [22] and formation of quasicrystal by physical vapor deposition [23]. Therefore, our spatial disturbance method of control of pattern formation is of general relevance.

We consider a general two-dimensional model in optics [19],

$$\partial_t \mathbf{q} = \mathbf{N}(\mathbf{q}, \mu) + iD\nabla_{\perp}^2 \mathbf{q}, \quad (1)$$

where  $\mathbf{q}$  is the vector variable,  $\mathbf{N}$  is a nonlinear function,  $t$  is time,  $D$  is the matrix of diffractive coefficients, and  $\nabla_{\perp}^2$  is the transverse Laplacian.  $\mu$  is the control parameter of the system, to which, in our stabilizing algorithm, the spatial perturbation is exerted, i.e.,

$$\mu = \mu_0[1 + \alpha f(x, y)], \quad (2)$$

where  $\mu_0$  is the unperturbed control parameter,  $\alpha$  is the amplitude of the perturbation, and  $f(x, y)$  is the spatial perturbation function. Here  $\alpha$  should be much smaller than one. The function  $f(x, y)$  should be designed to reflect the signature of the target pattern. The most natural form of  $f(x, y)$  is, therefore, chosen as that of the basic harmonics of the target pattern, which is the reminiscence of the widely used modulational control of temporal chaos [8–14]. For a demonstration of our technique, we consider the mean-field model for a two-level atomic medium in an optical cavity [24,25],

$$\begin{aligned} \partial_t E = -E \left[ (1 + i\theta) + \frac{2C(1 - i\Delta)}{|E|^2 + 1 + \Delta^2} \right] \\ + E_I + i(\partial_{xx} + \partial_{yy})E, \end{aligned} \quad (3)$$

where  $E$  is the intracavity electric field,  $\theta$  is the cavity detuning,  $\Delta$  is the atomic detuning,  $C$  is the optical absorptivity, and  $E_I$  is the pump field. For simplicity we restrict ourselves to the atomic resonance ( $\Delta = 0$ ) and the

plane-wave pump case and fix the cavity detuning to  $\theta = -1$  [21]. In this case, Eq. (3) has stationary, homogeneous solutions  $E_S$  given by [25]

$$\frac{E_I}{E_S} = 1 + i\theta + \frac{2C}{|E_S|^2 + 1}. \quad (4)$$

We choose the pump field  $E_I$  and the optical absorptivity  $C$  as two control parameters. Considering the experimental feasibility we apply the spatial perturbation to the pump field. Corresponding to Eq. (2), the perturbed pump field  $E_I$  can be written as

$$E_I = E_{I0}[1 + \alpha f(\mathbf{r})], \quad (5)$$

where  $E_{I0}$  is the unperturbed pump field. Previous analytical and numerical works [21,25] have shown that in this system the steady state consists of two (roll), four (square), or six (hexagon) equally spaced spatial modes. All the unstable patterns we will stabilize with our control can be constructed using eight wave vectors  $\mathbf{K}_i$  ( $i = 1, 2, \dots, 8$ ) with the same magnitude and arbitrary absolute orientations [21]. Therefore, for the case of rolls, the perturbation control function  $f(\mathbf{r})$  can be written as

$$f(\mathbf{r}) = \frac{1}{2}[e^{i(\mathbf{K}_1 \cdot \mathbf{r} + \phi_1)} + \text{c.c.}], \quad (6)$$

where  $\phi_1$  is an arbitrary phase. For the case of squares, it can be written as

$$f(\mathbf{r}) = \frac{1}{2}[e^{i(\mathbf{K}_1 \cdot \mathbf{r} + \phi_1)} + e^{i(\mathbf{K}_3 \cdot \mathbf{r} + \phi_3)} + \text{c.c.}], \quad (7)$$

where the wave vectors  $\mathbf{K}_1$  and  $\mathbf{K}_3$  are mutually perpendicular and the phases  $\phi_1$  and  $\phi_3$  are arbitrary. And for the two types of hexagonal patterns,  $H^+$  and  $H^-$ , it can be written as

$$f(\mathbf{r}) = \frac{1}{2}[e^{i(\mathbf{K}_1 \cdot \mathbf{r} + \phi_1)} + e^{i(\mathbf{K}_4 \cdot \mathbf{r} + \phi_4)} + e^{i(\mathbf{K}_6 \cdot \mathbf{r} + \phi_6)} + \text{c.c.}], \quad (8)$$

where  $\mathbf{K}_1$ ,  $\mathbf{K}_4$ , and  $\mathbf{K}_6$  make an angle of  $2\pi/3$  with each other. For  $H^+$  hexagons with intensity peaks we have  $\phi_1 + \phi_4 + \phi_6 = 2n\pi$ . For  $H^-$  hexagons or honeycombs consisting of intensity dips we have  $\phi_1 + \phi_4 + \phi_6 = (2n + 1)\pi$ .

The results which we will present were obtained by numerically integrating Eq. (3) with the spatially perturbed pump defined in Eq. (5). The integrations were performed using a split step spectral method on a  $64 \times 64$  grid with a box size of  $16\pi/K_c$  unless otherwise noted. Here  $K_c = \sqrt{-\theta}$ . We fix the control parameter  $C = 4.4$  (the minimum of the pattern forming threshold is at  $C = 4$ ). For different values of  $I = |E_S|^2$ , the unstable patterns of roll, square, and hexagons ( $H^+$  and  $H^-$ ) [21] are stabilized with the control function defined in Eqs. (6), (7), and (8), respectively, as shown in Fig. 1. It can be seen that the control is very successful with the perturbation amplitude as small as  $\alpha = 0.01$ . With our control technique it is very easy to select the unstable pattern from some local regions of the whole field. Two examples are shown in Fig. 2 where in Fig. 2(a) the perturbation is exerted to the left-hand half of the pump

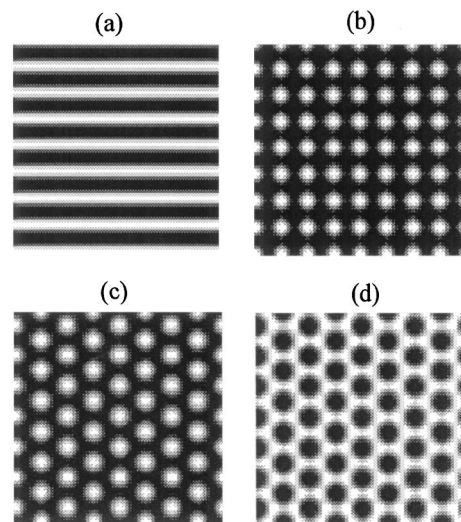


FIG. 1. Stabilized patterns with  $\alpha = 0.01$ : (a) Rolls and (b) squares for the case of coexistence of unstable rolls, squares, and  $H^-$  hexagons with stable  $H^+$  hexagons for  $I = 2.2$ , (c)  $H^+$  hexagons for the case of coexistence of unstable  $H^+$  hexagons and squares with stable  $H^-$  hexagons and rolls for  $I = 4.5$ , (d)  $H^-$  hexagons for the case of coexistence of unstable  $H^-$  hexagons and squares with stable  $H^+$  hexagons and rolls for  $I = 3.2$ .

field and in Fig. 2(b) only the central circular region (with the diameter of  $16\pi/K_c$ ) is controlled. We can see that the unstable rolls inside the controlled region are extracted from the uncontrolled hexagonal background.

The dynamics of the control process can be seen from the temporal evolution of the Fourier spectra, as shown in Fig. 3, where the perturbation function of Eq. (6) for stabilizing the rolls is exerted to the system at time  $t = 0$  after the stable uncontrolled hexagonal pattern is attained. We can see that the control process is accompanied with the suppression of the undesired modes and the enhancement of the desired modes. In order to present a quantitative description for the transient process, we calculated the decay time of the suppressed modes in the

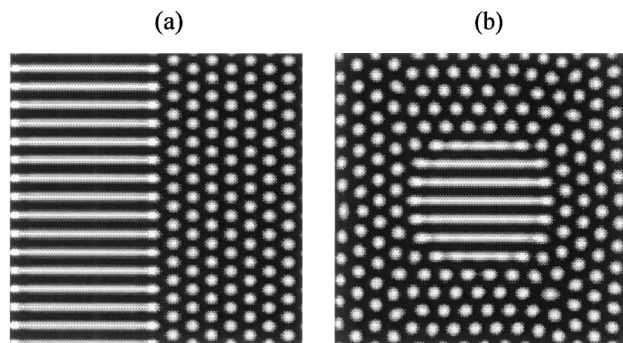


FIG. 2. Locally stabilized rolls for the case of coexistence of unstable rolls, squares, and  $H^-$  hexagons with stable  $H^+$  hexagons for  $I = 2.2$  with  $\alpha = 0.01$ , where a  $128 \times 128$  grid with a box size of  $32\pi/K_c$  is used.

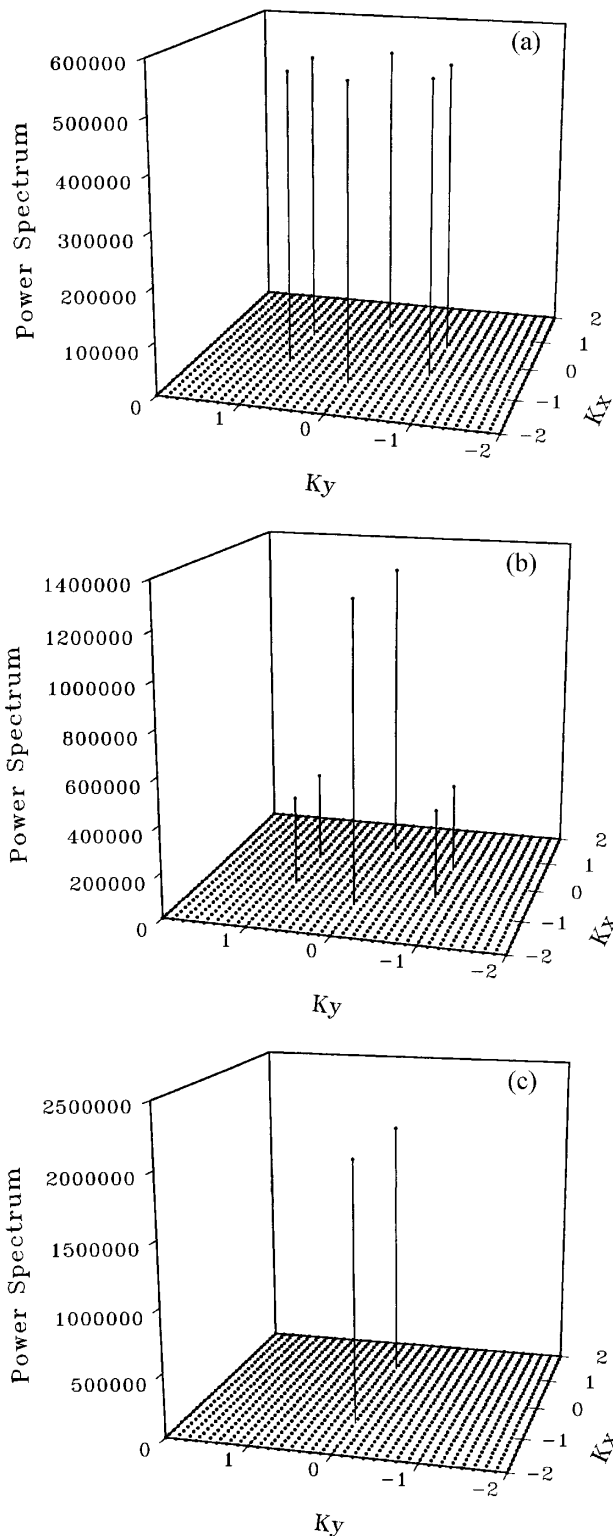


FIG. 3. Fourier spectrum at time (a)  $t = 0$ , (b)  $t = 100$ , and (c)  $t = 500$  for stabilizing the rolls for  $I = 2.2$  with  $\alpha = 0.005$ . The large component at the center is removed for clarity.

case of selecting rolls from the unperturbed hexagons. The time when the intensity of the undesired modes decay

to  $10^{-5}$  of its initial value is defined as the characteristic transient time  $t_0$ . It is straightforward to imagine that the larger the perturbation amplitude  $\alpha$  is, the shorter the transient time  $t_0$  will be, and, on the contrary, when the perturbation amplitude  $\alpha$  is smaller than a critical value  $\alpha_c$ , the control will fail; in other words, at  $\alpha_c$  the transient time  $t_0$  becomes infinity. This assertion is confirmed by the calculation of  $t_0$  versus  $\alpha$  as shown in Fig. 4. By fitting the result with the critical slowing down relation  $t_0 \propto (\alpha - \alpha_c)^{-\beta}$ , we obtain the critical perturbation amplitude  $\alpha_c \approx 0.0047025$  and the critical exponent  $\beta \approx 0.3541182$ . The excellent fit, as shown in Fig. 4, implies a perfect critical behavior. The small value of  $\alpha_c$  means that even a very weak perturbation is enough to control the formation of the pattern.

Up to now, all the simulations are performed with the spatial perturbations with a fixed magnitude of the wave vector  $\mathbf{K}$ , i.e.,  $|\mathbf{K}| = K_C = \sqrt{-\theta}$ . In order to see whether there exists a resonance phenomenon with the perturbation, we slightly change the magnitude of the perturbation wave vector around  $K_C$ . The phase diagram for tracking the rolls in the  $K$ - $\alpha$  plane is shown in Fig. 5. It is clear that the spatially resonant interactions play an important role, which is a reminiscence of the temporal parametric resonance phenomenon [26] where the resonant regions form Arnold tongues.

In addition to the perturbations applied to the amplitude of the pump field, we also realized the control by applying a spatial perturbation to the phase of the pump field, i.e., using

$$E_I = E_{I0} e^{i\alpha f(\mathbf{r})} \tag{9}$$

instead of Eq. (5). For example, we successfully stabilized the rolls for  $I = 2.2$  and  $\alpha = 0.02$  with Eq. (9).

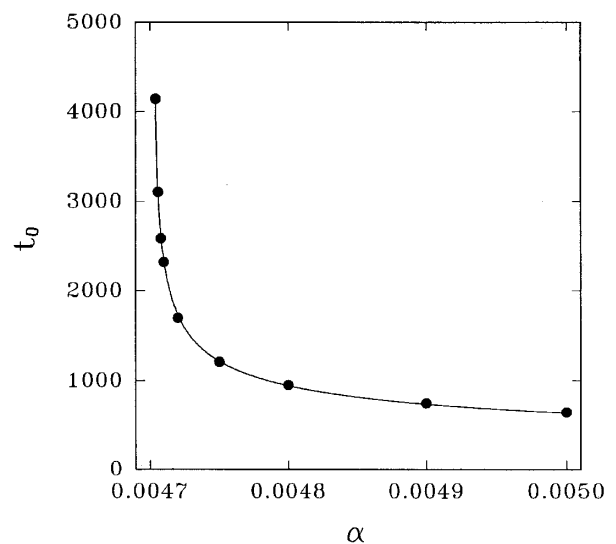


FIG. 4. Decay time  $t_0$  of the undesired modes versus  $\alpha$  for stabilizing the rolls for  $I = 2.2$ .

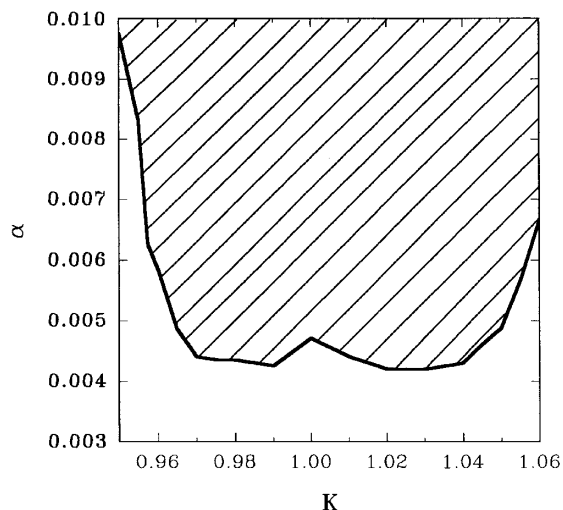


FIG. 5.  $K$ - $\alpha$  phase diagram for stabilizing the rolls for  $I = 2.2$ , where the shaded and blank areas are controllable and uncontrollable regions, respectively.

In summary, we have presented a spatial perturbation method to select, stabilize, and track unstable patterns. The perturbation, as a weak driving signal, mimics the target pattern. The method has been applied successfully to a nonlinear optical system. The application of the weak spatial perturbation results in the suppression of the undesired modes in the formation process of the target pattern. Detailed simulations reveal critical slowing down and resonant phenomenon.

This research was supported by the National Natural Science Foundation of China and by the Nonlinear Science Project of China.

- 
- [1] E. Ott, C. Grebogi, and J.A. Yorke, *Phys. Rev. Lett.* **64**, 1196 (1990).
  - [2] W.L. Ditto, S.N. Rauseo, and M.L. Spano, *Phys. Rev. Lett.* **65**, 3211 (1990); U. Dressler and G. Nitsche, *ibid.* **68**, 1 (1992).
  - [3] B. Peng, V. Petrov, and K. Showalter, *J. Phys. Chem.* **95**, 4957 (1991).
  - [4] E.R. Hunt, *Phys. Rev. Lett.* **67**, 1953 (1991); R. Roy, T.W. Murphy, T.D. Maier, Z. Gills, and E.R. Hunt, *ibid.* **68**, 1259 (1992).

- [5] P. Parmananda, P. Sherard, R.W. Rollins, and H.D. Dewald, *Phys. Rev. E* **47**, R3003 (1993).
- [6] K. Pyragas, *Phys. Lett. A* **170**, 421 (1992); K. Pyragas and A. Tamasevicius, *ibid.* **180**, 99 (1993).
- [7] W. Just, T. Bernard, M. Ostheimer, E. Reibold, and H. Benner, *Phys. Rev. Lett.* **78**, 203 (1997).
- [8] R. Lima and M. Pettini, *Phys. Rev. A* **41**, 726 (1990).
- [9] Y. Braiman and I. Goldhirsch, *Phys. Rev. Lett.* **66**, 2545 (1991).
- [10] A. Azevedo and S.M. Rezende, *Phys. Rev. Lett.* **66**, 1342 (1991).
- [11] L. Fronzoni, M. Giocondo, and M. Pettini, *Phys. Rev. A* **43**, 6483 (1991).
- [12] R. Chacón and J. Díaz Bejarano, *Phys. Rev. Lett.* **71**, 3103 (1993).
- [13] R. Meucci, W. Gadoski, M. Ciofini, and F.T. Arecchi, *Phys. Rev. E* **49**, R2528 (1994).
- [14] P. Colet and Y. Braiman, *Phys. Rev. E* **53**, 200 (1996).
- [15] J.A. Sepulchre and A. Babloyantz, *Phys. Rev. E* **48**, 945 (1993).
- [16] G. Hu and Z.L. Qu, *Phys. Rev. Lett.* **72**, 68 (1994); D. Auerbach, *ibid.* **72**, 1184 (1994).
- [17] F. Qin, E.E. Wolf, and H.C. Chang, *Phys. Rev. Lett.* **72**, 1459 (1994); I. Aranson, H. Levine, and L. Tsimring, *ibid.* **72**, 2561 (1994); V. Petrov, S. Metens, P. Borckmans, G. Dewel, and K. Showalter, *ibid.* **75**, 2895 (1995); A. Hagberg, E. Meron, I. Rubinstein, and B. Zaltzman, *ibid.* **76**, 427 (1996).
- [18] G.A. Johnson, M. Löcher, and E.R. Hunt, *Phys. Rev. E* **51**, R1625 (1995); C. Lourenço, M. Hougardy, and A. Babloyantz, *ibid.* **52**, 1525 (1995).
- [19] W. Lu, D. Yu, and R.G. Harrison, *Phys. Rev. Lett.* **76**, 3316 (1996).
- [20] M.C. Cross and P.C. Hohenberg, *Rev. Mod. Phys.* **65**, 851 (1993).
- [21] R. Martin, A.J. Scroggie, G.-L. Oppo, and W.J. Firth, *Phys. Rev. Lett.* **77**, 4007 (1996).
- [22] L.C. Jorritsma, M. Bijnagte, G. Rosenfeld, and B. Poelsema, *Phys. Rev. Lett.* **78**, 911 (1997).
- [23] T. Eisenhammer and A. Trampert, *Phys. Rev. Lett.* **78**, 262 (1997).
- [24] L.A. Lugiato and C. Oldano, *Phys. Rev. A* **37**, 3896 (1988).
- [25] W.J. Firth and A.J. Scroggie, *Europhys. Lett.* **26**, 521 (1994).
- [26] F.J. Romeiras and E. Ott, *Phys. Rev. A* **35**, 4404 (1987).